Effect of Pressure on the Dynamics of Iodide Defects in Methylammonium Lead Iodide: An Atomistic Simulation

THE JOURNAL OF PHYSICAL CHEMISTRY C
A JOURNAL OF THE AMERICAN CHEMICAL SOCIETY

pubs.acs.org/JPCC
Article

Effect of Pressure on the Dynamics of Iodide Defects in Methylammonium Lead Iodide: An Atomistic Simulation

Rachel Elizabeth Brophy,* Movaffaq Kateb, Kristinn Torfason, George Alexandru Nemnes, Halldor Gudfinnur Svavarsson, Ioana Pintilie, and Andrei Manolescu

Cite This: J. Phys. Chem. C 2023, 127, 7938−7943

ABSTRACT: The diffusion of iodide defects has been considered the most important degradation mechanism of methylammonium lead iodide (MAPI) in solar cells. The present study demonstrates the importance of the pressure inside this material on the dynamics of iodide defects, using molecular dynamics simulations. It is known that the diffusion coefficient of an iodide vacancy is an order of magnitude higher than that of interstitial iodide. We show that this difference systematically increases with increased tensile strain and that both diffusion coefficients tend to zero when a compressive strain is applied. This result suggests that compression of the MAPI can be a good solution to reduce its degradation rate. Besides, the statistical aspect of deriving the diffusion coefficient from the mean squared displacement (MSD) is discussed in terms of the initial conditions (positions and velocities) of the atoms and the simulation time, considering different seeds of the pseudorandom number generator used in the simulations performed with the LAMMPS software.

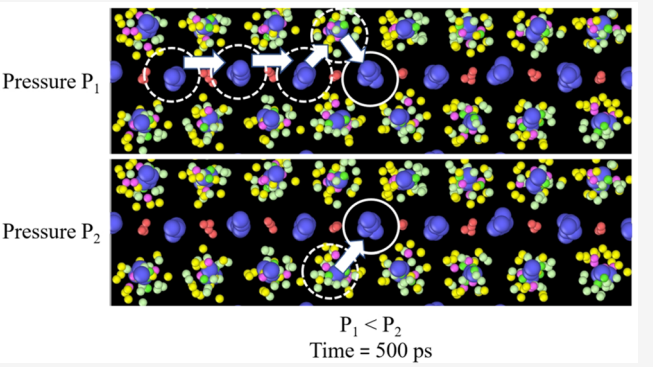

INTRODUCTION

Methylammonium lead iodide (MAPI)[1] is a promising photovoltaic material mainly due to its low-cost fabrication and high power conversion efficiency, exceeding 24%.[2] It has a perovskite structure with $CH_3NH_3PbI_3$ stoichiometry in which the methylammonium (MA) molecule, or CH_3NH_3, has a 1:1 ratio with Pb and is located in the middle of a nearly cubic cell made of PbI_3. Then the structure polymorphism is dominated by the kinetics of MA molecules; i.e., their random rotation gives the cubic phase ($Pm\bar{3}m$), while more aligned molecules lead to tetragonal ($I4/mcm$) and orthorhombic ($P4/mbm$) phases. However, the MAPI material is currently characterized by the lack of stability and relatively short lifetime in the working conditions of a solar cell. It has been found that diffusion of the negatively charged iodine ion, also known as iodide, is the primary degradation mechanism of the MAPI cell.[3−6] Moreover, the iodide migration and accumulation at the interfaces with the charge transport layers lead to a hysteretic behavior of the current−voltage characteristic of the device.[7−9]

In order to describe the behavior of the MAPI cells with atomistic simulations, and in particular the iodide migration, a simple but useful interatomic force field, called MYP, has recently been developed.[10] This force field allows modeling several thermodynamic properties of MAPI via molecular dynamics (MD) simulations.[11] Using the MYP potential, the variation of defect dynamics with temperature could be simulated.[12] The motion of defects near grain boundaries was compared with experimental data,[13] and strain introduced by an external electric field due to caloric effects has been studied.[14] It has been shown that hydrostatic pressure can affect the optical, electronic, and photovoltaic properties of various hybrid perovskites.[15−21] Earlier, it was shown that the diffusion barrier changes with variation of the lattice constant, which can be achieved by applying an external strain or by alloying MA and I sites.[22]

The MYP potential has been verified to reproduce *ab initio* results regarding the rotational dynamics of the MA cation and the phase transition in MAPI.[10,11,23] These properties are achieved by using the Lennard-Jones potential for the interaction of H atoms of the MA with the cage atoms and Buckingam−Coulomb for the interaction of C and N with the cage. The Lennard-Jones potential allows the orientation of the MA, while the Buckingam−Coulomb fixes its center of mass.

Received: January 30, 2023
Revised: April 3, 2023
Published: April 21, 2023

https://doi.org/10.1021/acs.jpcc.3c00657
J. Phys. Chem. C 2023, 127, 7938−7943

The diffusion coefficient obtained with MYP is also compatible with that from the experimental results.[24,25]

In the present study, we utilize the MD method to determine the effect of pressure on the iodide defect dynamics in MAPI. We consider separately the motion of an iodide vacancy and of an interstitial iodide ion. Apart from the presence of the defect, the MAPI material is assumed to be homogeneous.

METHODS

We performed our simulation with the LAMMPS software package[26] which solves Newton's equation of motion based on parametrized interatomic forces, which were derived from the MYP potential.[10] The intra-MA interactions are modeled with a bounded generalized Amber force field (GAFF). Pb−Pb, I−I, Pb−I, and Pb/I−C/N interactions are considered nonbonded and modeled with the Buckingham force field. Pb/I−H interactions were modeled by Lennard-Jones potential. Partial charges are assigned to each atom species and associated with pairwise Coulomb potentials. The Coulomb interaction was calculated in real space up to a 10 Å cutoff. The contribution beyond this cutoff was computed in the *k*-space. For the latter we utilized the Ewald summation with a particle−particle particle−mesh (pppm) solver and an accuracy of 10^{-4}.

The initial defect-free MAPI structure was considered to be orthorhombic, with a simulation cell consisting of 3072 atoms which correspond to 8 × 8 × 4 = 256 cubic unit cells. We assumed the *c*-axis of the orthorhombic crystal in the *z* direction which leaves the basal plane (*ab*) of the crystal parallel to the *xy* plane, as shown in Figure 1.

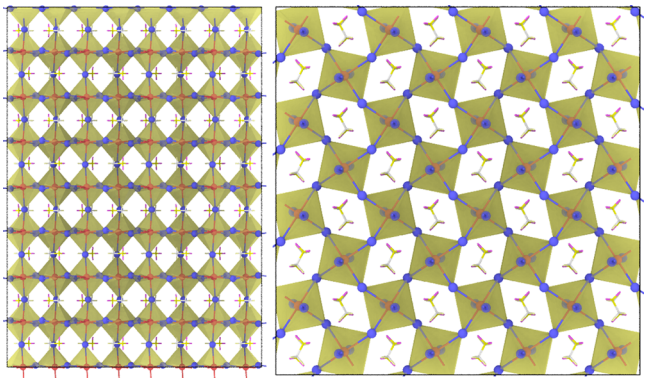

Figure 1. (left) *b*- and (right) *c*-Axis views of the initial structure of defect-free MAPI. Each Pb atom in red is surrounded by 6 I atoms that together form octahedra indicated by yellow. Note how MA molecules are oriented within empty spaces between octahedra in the *c*-axes view.

The system was relaxed in three steps. First, an energy minimization was performed using the conjugate gradient algorithm with a tolerance of 10^{-6} Kcal/mol Å for the force and 10^{-8} relative tolerance for the energy ($\Delta E/E$). We allowed the box dimension to vary during the minimization to produce the desired pressure, between -5×10^3 and 10^5 bar. The latter is more efficient than performing NPT since it does not rescale temperature; instead, it includes $P\Delta V$ and Parrinello and Rahman[27] strain energy during the energy minimization. Further relaxation was performed using the isothermal−isobaric (NPT) ensemble, by performing a temperature and pressure rescaling at each 100-th and 500-th time step (with every single step of 0.5 fs), using the Noose−Hoover thermostat and barostat, respectively. We gradually increased the temperature from 1 to 300 K within a time interval of 0.25 ns, and maintained it constant for an interval of 1.75 ns. Then, the same NPT ensemble was used for the subsequent part of the simulation. The typical computational time was about 22 CPU hours for each nanosecond on a high-performance computer cluster of AMD EPYC processors at 2300 MHz.

In practice, MAPI suffers from a relatively high density of various defects originating in the preparation process, most often in the original chemical solution used. In the present work, we consider two types of iodide defects: iodide vacancy and iodide interstitial. They can be generated simply by removing or adding an iodide to the lattice, respectively. They are both considered positively and negatively charged, respectively, and therefore, theoretically, these defect models may slightly violate the charge neutrality of the entire system. However, if the total number of atoms is sufficiently large, there should be no practical consequence on the atomistic simulations.[12] Instead, a paired iodide-vacancy defect can also be created by displacing an iodide from its original site to a desired distance. This model allows for maintaining the charge neutrality of the system, but it may not be viable for a long time as the pair may recombine. Nevertheless, implicit charge neutralization of the cell has been implemented in the *k*-space solver, where a neutralizing background was taken into account by excluding the energy corresponding to $k = 0$ from the lattice sum.

In order to observe the diffusion of the iodide defects, we compute the time-dependent mean square displacement (MSD) of all iodide ions during the simulation, which is

$$\mathrm{MSD}(t) = \frac{1}{N_\mathrm{I}} \sum_{i=1}^{N_\mathrm{I}} |\mathbf{r}_i(t) - \mathbf{r}_i(0)|^2 \tag{1}$$

where N_I is the total number of all iodide ions in our simulation cell, and $\mathbf{r}_i(t)$ is the position of each iodide ion, $i = 1, 2, ..., N_\mathrm{I}$, at time *t*. In the absence of mobile atoms, the MSD varies only due to the local thermal vibration, with a small average over the entire simulation time. Instead, the presence of mobile defects leads to a linear trend of MSD versus time, with a positive slope. Using the random walk theory the diffusion coefficient *D* of the mobile defect can be calculated as[28]

$$D = \frac{1}{6} \lim_{t\to\infty} \frac{\mathrm{MSD}(t)}{t} \tag{2}$$

In practice *D* can be obtained as the slope coefficient of the MSD versus time, divided by the factor 6, which is the double of the spatial dimension.[11,12] The relaxation time after the initial positions, plus an additional extra time after that, is excluded from the slope calculation.

We utilized the open visualization tool (OVITO) and its Python interface for postprocessing and visualization.[29]

RESULTS

Iodide Vacancy. Figure 2 shows the time-dependent MSD and the corresponding diffusion coefficients *D* for an iodide vacancy at 300 K and different applied pressures. It can be seen that the negative pressures, corresponding to a tensile strain (and an expansion of the material), lead to an increased slope of the MSD and of the corresponding diffusion coefficient, while in the presence of a positive pressure (or a compression

https://doi.org/10.1021/acs.jpcc.3c00657
J. Phys. Chem. C 2023, 127, 7938−7943

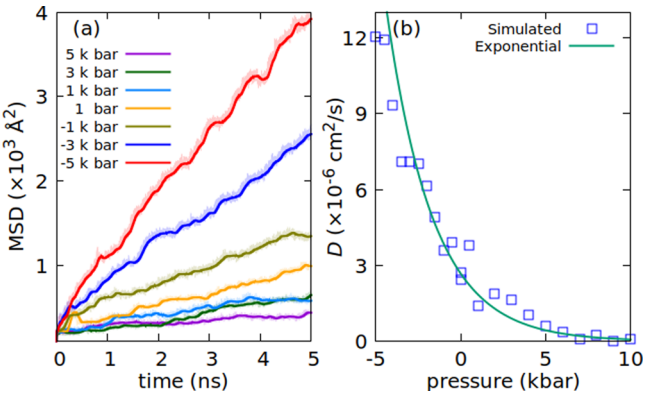

Figure 2. (a) MSD of iodide vacancy at 300 K and different pressures. The lines show a smeared MSD using 2000 time points, while the original data is shown as a shaded area around the lines. (b) Variation of D with pressure for more values of the pressure, the solid line being the exponential fit mentioned in the main text.

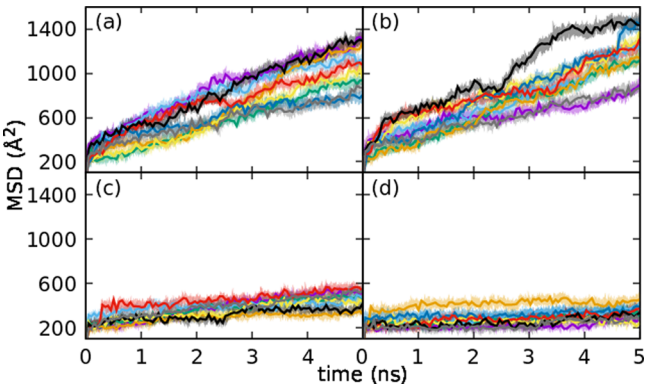

Figure 3. (a) MSD in the presence of an iodide vacancy, at a pressure of 1 bar, using different seeds of the random number generator and (b) also using different initial positions of the vacancy. (c,d) The same at pressure 5 kbar. The temperature was fixed at 300 K.

of the material), the diffusion coefficient decreases and eventually tends to zero at about 10 kbar (not shown). (More on the sign of the pressure is given in the Supporting Information.)

The graph clearly indicates an exponential decrease of D with increasing pressure p. A linear fit of the resulting values of the diffusion coefficient of the iodide vacancy, on the log scale, yielded an R-squared coefficient of 0.92. The corresponding solid line shown in Figure 2(b) is the resulting fitting function, $2.67 \times 10^{-6}\exp(-0.364\ p)$. At atmospheric pressure our diffusion coefficient is 2.42×10^{-6} cm^2/s, close to the value reported by Delugas et al., which is 4.3×10^{-6} cm^2/s, obtained at 300 K but using the canonical thermodynamic ensemble, NVT, implemented in the DL_POLY molecular simulation package.[12] The decrease of the MSD and of the diffusion coefficient with increasing pressure can be associated with the increase of the density of the MAPI material, leading to a blocking of the iodide atoms at their original sites or to an increase of the energy they need for jumping into the nearby vacancy. Delugas et al.[12] also estimated the activation energy of the iodide interstitial and vacancy at atmospheric pressure, to 0.24 and 0.1 eV, respectively, whereas the experimental results for the iodide ion range between 0.3 and 0.6 eV.[30] To our knowledge, a systematic study of these activation energies as a function of pressure has not been performed.

As we can see in Figure 2(a), the instantaneous time derivative of the MSD, $d(\mathrm{MSD})/dt$, is not a smooth function of time. For this reason, for a reasonably accurate estimation of the diffusion coefficient D, a simulation time longer than the average oscillation time of the MSD slope is needed, and apparently, a total time of several ns should be sufficient. However, the observable variation of the slope, over shorter time intervals, also suggests that the MSD evolution may depend on the initial conditions. To check that we repeated the simulations by changing the seed of the (pseudo)random number generator in LAMMPS, which implies different initial states of the entire lattice at the beginning of the simulation, and also after the relaxation phase, and consequently different trajectories of the entire system in the phase space. In addition, we also used different (random) initial placements for the vacancy.

Figure 3(a,c) shows the MSD results for the iodide vacancy with different seeds at 1 bar and 5 kbar, respectively. In both cases, the initial positions of all atoms were the equilibrium positions plus random displacements with $-0.1 < \delta < 0.1$ Å in each direction x, y, z, depending on the seed. The initial velocities of the atoms were also assigned randomly, from a Gaussian distribution, again depending on the seed. Thus, all simulations began with different initial conditions. Additionally, in Figure 3(a,c) the iodide vacancy had the same initial position, whereas in Figure 3(b,d) this position was also randomized. Clearly, the effect of the seed creates significant variations of the slope. This is evident at both pressures used. We can also see that at the higher pressure of 5 kbar the slope is systematically reduced, in agreement with the previous result that the diffusion of iodide vacancies is suppressed at elevated pressures.

In the nine simulations represented in Figure 3(a), at 1 bar, the slope coefficients are, in increasing order: 96, 104, 151, 159, 163, 179, 189, 204, and 229 Å^2/ns, with a mean value of 164 Å^2/ns and a standard error (or statistical uncertainty) of about 14 Å^2/ns, meaning ±9% relative uncertainty for the estimated diffusion coefficient. With the data obtained at 5 kbar the relative uncertainty of D is about ±15%. At the same time, the uncertainty of the slope coefficient corresponding to a single simulation is much smaller, in the range 0.1−0.3% or less, because it is based on a sample with millions of time points.

Therefore, it turns out that every single run of several ns does not include sufficient information about the distribution of all possible states of the system in the phase space. This is true because the slope coefficients obtained with 4 ns simulations differ from their mean values obtained with different initial conditions. It is also seen in our figures that the slope of the MSD vs time changes on intervals of the order of 1 ns or less. Similar slope variations can also be observed in the calculations of Delugas et al., in their Figure 3, representing the MSD data for iodide vacancy and iodide interstitial at different temperatures.[12] Our interpretation is that a computational time of several ns is not sufficient to observe the ergodic behavior of our system, i.e., the convergence of the time-averaged and phase space-averaged values of the diffusion coefficient. For that purpose, an unrealistically long computational time might be necessary, or instead, a reasonable accuracy could be achieved with shorter simulations with different initial conditions. Long-time memory of initial conditions in a diffusion process has also been addressed by

https://doi.org/10.1021/acs.jpcc.3c00657
J. Phys. Chem. C 2023, 127, 7938−7943

other studies and formulated on a rigorous mathematical background.[31] However, such fundamental aspects of statistical mechanics are beyond the scope of our present work and rather are based on an empirical approach.

Iodide Interstitial. Now we consider an interstitial iodide ion added to the MAPI lattice and repeat the previous simulations. The results are shown in Figure 4, obtained with

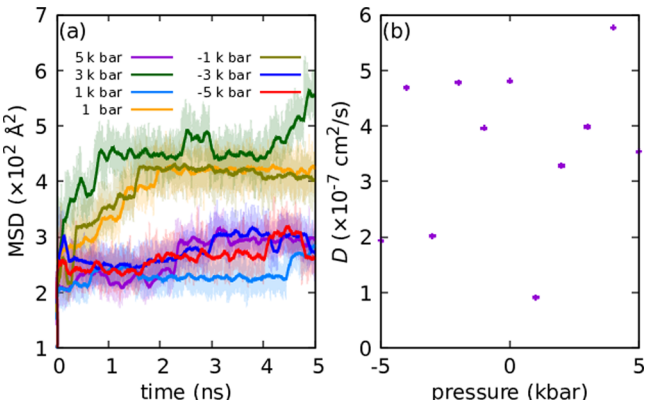

Figure 4. (a) MSD of the iodide interstitial at 300 K and different pressures. Darker lines indicate a moving average of 2000 points, while the original data are shown with lighter colors in the background. (b) Variation of D with pressure.

the NPT ensemble, at different pressures. As before, the MSD corresponds to all iodide ions, and the diffusion coefficient of the interstitial ion is found from the slope of the MSD. Note that the scale of the diffusion coefficient D is an order of magnitude smaller than in the case of the vacancy (Figure 2(b)). Again, we are close to the value previously reported by Delugas et al. of 7.4×10^{-7} cm^2/s, obtained using the NVT ensemble at 300 K.[12] We also found that the diffusion coefficient of the interstitial iodide is at least 1 order of magnitude smaller than that of the vacancy at atmospheric pressure.

However, in the iodide case, we could not find a systematic variation of the diffusion coefficient with the applied pressure. The values shown in Figure 4(b) are scattered and probably not convergent after the 5 ns simulation time. The slope of the MSD data now looks variable over larger time intervals than in the case of the vacancy, and as expected, by repeating the simulations with different seeds of the random number generator, the overall slope of MSD with respect to time is systematically smaller than in the case of the iodide vacancy and possibly with a larger uncertainty.

The results obtained with different seeds, for pressures of 1 bar and 5 kbar, are shown in Figure 5. It is clearly seen that when a defect is introduced in the same place (Figure 5(a,c)) the MSD data look similar and nearly flat. However, as can be seen in Figure 5(b,d), introducing the defect elsewhere might lead to different MSD data, but their slope is always much smaller than in the case of the vacancy. Nonetheless, the pressure seems to have a minor effect in these MSDs, indicating that iodide diffusion is a less frequent event, at least up to a pressure of 5 kbar, which was our largest value.

To clarify these results, ten times longer simulations were performed for the case with the interstitial iodide, at four different pressure values. The resulting MSDs are shown in Figure 6. Note that the results corresponding to different pressures are shifted vertically, for illustration purposes. At this

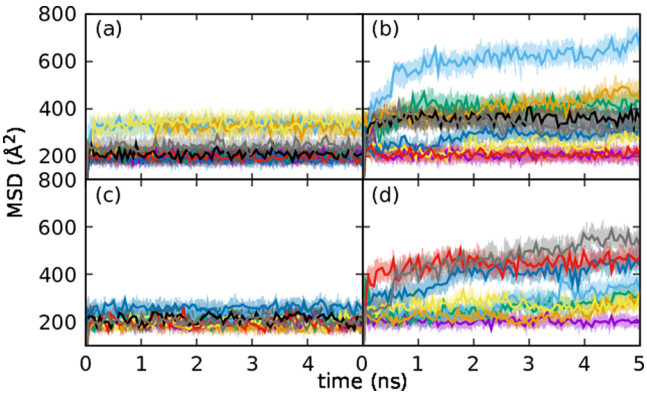

Figure 5. Variation of the MSD for the iodide interstitial with the seed of the random numbers. (a,b) Correspond to 1 bar and (c,d) to 5 kbar pressure. In (a) and (c) the initial position of the iodide was the same, whereas in (b) and (d) it was randomized.

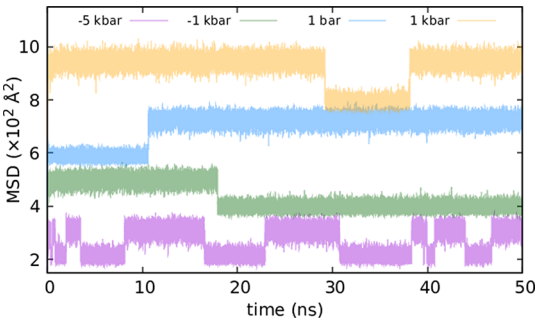

Figure 6. MSD of the iodide interstitial at different pressures obtained over a 50 ns time scale. The curves are shifted manually for clarity.

time scale, for all pressure values, we can only identify jumps of the MSD, on the background of all iodide ions' back-and-forth movements or local vibrations. The jumps are of approximately $\sqrt{\text{MSD}} \approx \sqrt{100} = 10$ Å, which correspond to the size of a unit cell. So at this time scale no net motion of the iodide can be identified, but only hopping events from one unit cell to another, which appear to be more frequent at high negative pressures such as −5 kbar than at positive pressures. However, a proper diffusion of the iodide interstitial may possibly be described on a longer time scale using the method of accelerated molecular dynamics.[32,33]

CONCLUSIONS

We performed molecular dynamics simulations of the iodide migration in the MAPI material, using the LAMMPS software, over time intervals from a few to a few tens of ns, and we obtained estimated values of the diffusion coefficients of the iodide vacancies and interstitial atoms for different negative and positive pressures applied to the MAPI material. Our simulations show that the iodide vacancy has a diffusion coefficient or, equivalently, a mobility that depends significantly on the pressure. The mobility of the vacancy varies exponentially with the pressure, increasing in the presence of tensile stress (negative pressure compared to the atmospheric value) and decreasing in the presence of compressive stress (positive pressure). For the same conditions, the mobility of an interstitial iodide is at least 1 order of magnitude lower, which means that the net, macroscopic, iodide migration can be associated with the diffusion of the iodide vacancies. Therefore the migration of the iodide, which is a major factor in the

https://doi.org/10.1021/acs.jpcc.3c00657
J. Phys. Chem. C 2023, 127, 7938−7943

degradation of the MAPI material, could be suppressed, or at least reduced, by applying to the material a compressive stress of the order of a few kbar.

Recent studies also suggested that with even larger pressures, of the order of hundreds of kbar, the band gap can also be modified, although achieving such pressures could be technically difficult and could possibly lead to phase transitions of the MAPI material.[34−36]

In our simulations, we assumed a homogeneous MAPI lattice and no external electric field. The presence of lattice defects such as grain boundaries can change the physical conditions. The local electric field may attract the ionic defects toward the grain boundaries,[13] inhibiting their diffusion further. However, the iodide migration may still occur at the contact between the MAPI material and another layer, for example, the hole transporter made of Spiro-OMeTAD.[6] Indeed, the degradation of MAPI occurs at a time scale much larger than our present simulations. The temperature in the working conditions, typically between 15 and 60 °C, is a contributing factor, but not the most important. Having an activation energy of tenths of eV, iodide vacancy generation can be initiated or triggered by photons. One can reduce the iodine accumulation and thus the degradation of the device by immobilizing the vacancies. This is typically achieved by passivation with inorganic or organic dopants.[37] Thermal treatment can increase the domain size of polycrystalline perovskites. Engineering halide composition, incorporating large organic cations, or introducing ionic additives are other strategies to mitigate ion migration.[38] In the present study, we are suggesting that a compressing stress could at least reduce the vacancy diffusion.

■ ASSOCIATED CONTENT

Supporting Information

The Supporting Information is available free of charge at https://pubs.acs.org/doi/10.1021/acs.jpcc.3c00657.

Additional details on determining the MSD of a vacancy and a brief description of negative pressure (PDF)

■ AUTHOR INFORMATION

Corresponding Author

Rachel Elizabeth Brophy − *Department of Engineering, Reykjavik University, IS-102 Reykjavik, Iceland;* orcid.org/0000-0002-5395-6861; Email: rachel18@ru.is

Authors

Movaffaq Kateb − *Department of Engineering, Reykjavik University, IS-102 Reykjavik, Iceland; Condensed Matter & Materials Theory Division, Department of Physics, Chalmers University of Technology, SE-412 96 Gothenburg, Sweden;* orcid.org/0000-0002-2518-3988

Kristinn Torfason − *Department of Engineering, Reykjavik University, IS-102 Reykjavik, Iceland;* orcid.org/0000-0002-4857-7840

George Alexandru Nemnes − *Research Institute of the University of Bucharest (ICUB), 050107 Bucharest, Romania; University of Bucharest, Faculty of Physics, 077125 Magurele-Ilfov, Romania; Horia Hulubei National Institute for Physics & Nuclear Engineering, 077126 Magurele-Ilfov, Romania;* orcid.org/0000-0002-8500-4953

Halldor Gudfinnur Svavarsson − *Department of Engineering, Reykjavik University, IS-102 Reykjavik, Iceland*

Ioana Pintilie − *National Institute of Materials Physics, 077125 Magurele-Ilfov, Romania;* orcid.org/0000-0002-3857-8524

Andrei Manolescu − *Department of Engineering, Reykjavik University, IS-102 Reykjavik, Iceland*

Complete contact information is available at: https://pubs.acs.org/10.1021/acs.jpcc.3c00657

Notes

The authors declare no competing financial interest.

■ ACKNOWLEDGMENTS

The research leading to these results has received funding from the EEA Grant 2014-2021, under Project contract no. 36/2021 (project code: EEA-RO-NO-2018-0106), and from the Core Program 2019-2022 (contract 21N/2019). R.E.B. is thankful for partial support from the National Power Company of Iceland (Landsvirkjun) via the Sustainability Institute and Forum (SIF) of Reykjavik University. The computational resource was sponsored by EGI and the EGI-ACE H2020 project (GA no. 101017567) with the dedicated support of CLOUDIFIN.

■ REFERENCES

(1) Kojima, A.; Teshima, K.; Shirai, Y.; Miyasaka, T. Organometal Halide Perovskites as Visible-Light Sensitizers for Photovoltaic Cells. *J. Am. Chem. Soc.* **2009**, *131*, 6050−6051.

(2) National Renewable Energy Laboratory (NREL). Best Research-Cell Efficiency Chart. https://www.nrel.gov/pv/cell-efficiency.html (accessed April 2nd 2022).

(3) Sanchez, R. S.; Gonzalez-Pedro, V.; Lee, J.-W.; Park, N.-G.; Kang, Y. S.; Mora-Sero, I.; Bisquert, J. Slow Dynamic Processes in Lead Halide Perovskite Solar Cells. Characteristic Times and Hysteresis. *J. Phys. Chem. Lett.* **2014**, *5*, 2357−2363.

(4) Eames, C.; Frost, J. M.; Barnes, P. R.; O'regan, B. C.; Walsh, A.; Islam, M. S. Ionic transport in hybrid lead iodide perovskite solar cells. *Nature communications* **2015**, *6*, 7497.

(5) Li, C.; Tscheuschner, S.; Paulus, F.; Hopkinson, P. E.; Kießling, J.; Köhler, A.; Vaynzof, Y.; Huettner, S. Iodine Migration and its Effect on Hysteresis in Perovskite Solar Cells. *Adv. Mater.* **2016**, *28*, 2446−2454.

(6) Besleaga, C.; Abramiuc, L. E.; Stancu, V.; Tomulescu, A. G.; Sima, M.; Trinca, L.; Plugaru, N.; Pintilie, L.; Nemnes, G. A.; Iliescu, M.; et al. Iodine Migration and Degradation of Perovskite Solar Cells Enhanced by Metallic Electrodes. *J. Phys. Chem. Lett.* **2016**, *7*, 5168−5175.

(7) Tress, W.; Marinova, N.; Moehl, T.; Zakeeruddin, S. M.; Nazeeruddin, M. K.; Grätzel, M. Understanding the rate-dependent J−V hysteresis, slow time component, and aging in $CH_3NH_3PbI_3$ perovskite solar cells: the role of a compensated electric field. *Energy Environ. Sci.* **2015**, *8*, 995.

(8) Zarazua, I.; Bisquert, J.; Garcia-Belmonte, G. Light-Induced Space-Charge Accumulation Zone as Photovoltaic Mechanism in Perovskite Solar Cells. *The Journal of Physical Chemistry Letters* **2016**, *7*, 525.

(9) Nemnes, G. A.; Besleaga, C.; Tomulescu, A. G.; Pintilie, I.; Pintilie, L.; Torfason, K.; Manolescu, A. Dynamic Electrical Behavior of Halide Perovskite Based Solar Cells. *Sol. Energy Mater. Sol. Cells* **2017**, *159*, 197−203.

(10) Mattoni, A.; Filippetti, A.; Saba, M. I.; Delugas, P. Methylammonium Rotational Dynamics in Lead Halide Perovskite by Classical Molecular Dynamics: The Role of Temperature. *The Journal of Physical Chemistry C* **2015**, *119*, 17421−17428.

(11) Mattoni, A.; Filippetti, A.; Caddeo, C. Modeling hybrid perovskites by molecular dynamics. *Journal of Physics: Condensed Matter* **2017**, *29*, 043001.

(12) Delugas, P.; Caddeo, C.; Filippetti, A.; Mattoni, A. Thermally Activated Point Defect Diffusion in Methylammonium Lead Trihalide: Anisotropic and Ultrahigh Mobility of Iodine. *The Journal of Physical Chemistry Letters* **2016**, *7*, 2356−2361.
(13) Phung, N.; Al-Ashouri, A.; Meloni, S.; Mattoni, A.; Albrecht, S.; Unger, E. L.; Merdasa, A.; Abate, A. The Role of Grain Boundaries on Ionic Defect Migration in Metal Halide Perovskites. *Advanced Energy Materials* **2020**, *10*, 1903735.
(14) Liu, S.; Cohen, R. Response of methylammonium lead iodide to external stimuli and caloric effects from molecular dynamics simulations. *The Journal of Physical Chemistry C* **2016**, *120*, 17274−17281.
(15) Kong, L.; Liu, G.; Gong, J.; Hu, Q.; Schaller, R. D.; Dera, P.; Zhang, D.; Liu, Z.; Yang, W.; Zhu, K.; et al. Simultaneous band-gap narrowing and carrier-lifetime prolongation of organic−inorganic trihalide perovskites. *Proceedings of the National Academy of Sciences* **2016**, *113*, 8910−8915.
(16) Jaffe, A.; Lin, Y.; Beavers, C. M.; Voss, J.; Mao, W. L.; Karunadasa, H. I. High-pressure single-crystal structures of 3D lead-halide hybrid perovskites and pressure effects on their electronic and optical properties. *ACS central science* **2016**, *2*, 201−209.
(17) Jaffe, A.; Lin, Y.; Karunadasa, H. I. Halide perovskites under pressure: accessing new properties through lattice compression. *ACS Energy Letters* **2017**, *2*, 1549−1555.
(18) Liu, G.; Kong, L.; Gong, J.; Yang, W.; Mao, H.-K.; Hu, Q.; Liu, Z.; Schaller, R. D.; Zhang, D.; Xu, T. Pressure-induced bandgap optimization in lead-based perovskites with prolonged carrier lifetime and ambient retainability. *Advanced Functional Materials* **2017**, *27*, 1604208.
(19) Wang, P.; Guan, J.; Galeschuk, D. T.; Yao, Y.; He, C. F.; Jiang, S.; Zhang, S.; Liu, Y.; Jin, M.; Jin, C.; et al. Pressure-induced polymorphic, optical, and electronic transitions of formamidinium lead iodide perovskite. *The Journal of Physical Chemistry Letters* **2017**, *8*, 2119−2125.
(20) Postorino, P.; Malavasi, L. Pressure-induced effects in organic−inorganic hybrid perovskites. *The journal of physical chemistry letters* **2017**, *8*, 2613−2622.
(21) Ghosh, D.; Aziz, A.; Dawson, J. A.; Walker, A. B.; Islam, M. S. Putting the squeeze on lead iodide perovskites: pressure-induced effects to tune their structural and optoelectronic behavior. *Chem. Mater.* **2019**, *31*, 4063−4071.
(22) Yang, D.; Ming, W.; Shi, H.; Zhang, L.; Du, M.-H. Fast diffusion of native defects and impurities in perovskite solar cell material CH3NH3PbI3. *Chem. Mater.* **2016**, *28*, 4349−4357.
(23) Mitran, T. L.; Brophy, R. E.; Cuzminschi, M.; Filipoiu, N.; Kateb, M.; Pintilie, I.; Manolescu, A.; Nemnes, G. A. *Low-Dimensional Halide Perovskites*; Elsevier, 2023; pp 153−185.
(24) Zhao, Y.; Zhou, W.; Han, Z.; Yu, D.; Zhao, Q. Effects of ion migration and improvement strategies for the operational stability of perovskite solar cells. *Phys. Chem. Chem. Phys.* **2021**, *23*, 94.
(25) Filipoiu, N.; Preda, A. T.; Anghel, D.-V.; Patru, R.; Brophy, R. E.; Kateb, M.; Besleaga, C.; Tomulescu, A. G.; Pintilie, I.; Manolescu, A.; et al. Capacitive and inductive effects in perovskite solar cells: the different roles of ionic current and ionic charge accumulation. *Physical Review Applied* **2022**, *18*, 064087.
(26) Plimpton, S. Fast parallel algorithms for short-range molecular dynamics. *Journal of computational physics* **1995**, *117*, 1−19.
(27) Parrinello, M.; Rahman, A. Polymorphic transitions in single crystals: A new molecular dynamics method. *Journal of Applied physics* **1981**, *52*, 7182−7190.
(28) Allen, M. P.; Tildesley, D. J. *Computer simulation of liquids*; Oxford university press: Oxford, 1989.
(29) Stukowski, A. Visualization and analysis of atomistic simulation data with OVITO−the Open Visualization Tool. *Modelling and simulation in materials science and engineering* **2010**, *18*, 015012.
(30) Ferdani, D. W.; Pering, S. R.; Ghosh, D.; Kubiak, P.; Walker, A. B.; Lewis, S. E.; Johnson, A. L.; Baker, P. J.; Islam, M. S.; Cameron, P. J. Partial cation substitution reduces iodide ion transport in lead iodide perovskite solar cells. *Energy & Environmental Science* **2019**, *12*, 2264−2272.
(31) Banerjee, T.; Jack, R. L.; Cates, M. E. Role of initial conditions in one-dimensional diffusive systems: Compressibility, hyperuniformity, and long-term memory. *Phys. Rev. E* **2022**, *106*, L062101.
(32) Sorensen, M. R.; Voter, A. F. Temperature-accelerated dynamics for simulation of infrequent events. *The Journal of Chemical Physics* **2000**, *112*, 9599−9606.
(33) Wang, Y.; Markwick, P. R. L.; de Oliveira, C. A. F.; McCammon, J. A. Enhanced Lipid Diffusion and Mixing in Accelerated Molecular Dynamics. *Journal of Chemical Theory and Computation* **2011**, *7*, 3199−3207.
(34) Rajeswarapalanichamy, R.; Amudhavalli, A.; Padmavathy, R.; Iyakutti, K. Band gap engineering in halide cubic perovskites CsPbBr3-yIy (y = 0, 1, 2, 3) - A DFT study. *Materials Science and Engineering: B* **2020**, *258*, 114560.
(35) Faghihnasiri, M.; Beheshtian, J.; Shayeganfar, F.; Shahsavari, R. Phase transition and mechanical properties of cesium bismuth silver halide double perovskites (Cs2AgBiX6, X = Cl, Br, I): a DFT approach. *Phys. Chem. Chem. Phys.* **2020**, *22*, 5959−5968.
(36) Lee, J.-H.; Jaffe, A.; Lin, Y.; Karunadasa, H. I.; Neaton, J. B. Origins of the Pressure-Induced Phase Transition and Metallization in the Halide Perovskite (CH3NH3)PbI3. *ACS Energy Letters* **2020**, *5*, 2174−2181.
(37) Maiti, A.; Chatterjee, S.; Peedikakkandy, L.; Pal, A. J. Defects and Their Passivation in Hybrid Halide Perovskites toward Solar Cell Applications. *Solar RRL* **2020**, *4*, 2000505.
(38) Bi, E.; Song, Z.; Li, C.; Wu, Z.; Yan, Y. Mitigating ion migration in perovskite solar cells. *Trends in Chemistry* **2021**, *3*, 575−588.

https://doi.org/10.1021/acs.jpcc.3c00657
J. Phys. Chem. C 2023, 127, 7938−7943